Lawrence Berkeley Laboratory

UNIVERSITY OF CALIFORNIA

Materials & Molecular Research Division

Submitted to Journal of Chemical Physics

Pt-Ti ALLOY FORMATION FROM HIGH TEMPERATURE REDUCTION OF A TITANIA IMPREGNATED Pt CATALYST: IMPLICATIONS FOR SMSI

B.C. Beard and P.N. Ross

September 1985

Prepared for the U.S. Department of Energy under Contract DE-AC03-76SF00098

DISCLAIMER

Pt-Ti ALLOY FORMATION FROM HIGH TEMPERATURE REDUCTION OF A TITANIA IMPREGNATED Pt CATALYST: IMPLICATIONS FOR SMSI

Bruce C. Beard and Philip N. Ross
Materials and Molecular Research Division
Lawrence Berkeley Laboratory
University of California
Berkeley, CA 94720

ABSTRACT

Highly dispersed Pt supported on carbon black was impregnated with titania and heated in an inert atmosphere. The amount of titania used was twice the stoichiometric amount required for the formation of the ordered alloy phase Pt_3Ti. The chemical state of the Ti at various stages of heating was determined by x-ray photoelectron spectroscopy and by extended x-ray absorption fine structure (EXAFS) analysis. The formation of alloy phases could also be determined by conventional x-ray diffraction methods. These characterizations showed unambiguously the conversion of separate Pt and TiO_2 dispersed phases into Pt-Ti alloy phases at progressively higher heat treatment temperatures, eventually resulting in the formation of crystallites of the ordered (intermetallic) phase Pt_3Ti. Based on this observation and other related work in the literature, we present a model for the chemistry occurring during the formation of the SMSI state of Pt/TiO_2 catalysts.

INTRODUCTION

We present the observation of Pt-Ti alloy formation when Pt supported on carbon black is impregnated with TiO_2 and heated in an inert atmosphere. This observation is of particular interest in its implications for the chemistry occurring in the strong metal support interaction (SMSI) between TiO_2 and the Group VIII metals. In the seminal SMSI paper by Tauster, Fung and Garten (1), three different mechanisms were suggested for the SMSI effect: Pt encapsulation by the support, poisoning by impurities, and alloy formation. Alloy formation was shown by Tauster, et al. to be at least thermodynamically possible under the high temperature reduction treatment used to produce the SMSI state. Following Brewer (2), they suggested that d-orbital bonding between the metals would be expected to change the adsorption properties of the Pt atoms. Horsley attempted to quantify the intermetallic bonding with SCF-X_α calculations of bonding of Pt to Ti^{+3} through oxygen vacancies (3). Experimentally, however, it has not been possible to determine whether in fact alloy formation occurs during the high temperature reduction of Pt dispersed on TiO_2. Both x-ray photoelectron

spectroscopy (XPS) and extended x-ray adsorption fine structure spectroscopy (EXAFS) are capable in principle of determining whether an alloy state forms, but when applied to the Pt/TiO_2 system there arise fundamental problems in detectability. In forming a Pt-Ti alloy, the largest changes in chemistry occur for the Ti atoms, e.g. from +4 with all oxygen nearest neighbors to near zero-valent with all Pt nearest neighbors, and chemical shifts in Ti core-levels and/or Ti K-edge EXAFS shifts are correspondingly large for these changes in the state of Ti. But the fraction of all Ti atoms present in the catalyst undergoing this change in chemistry is extremely small (about 1000:1 for 1% Pt on TiO_2) and the signal from the atoms undergoing the change is either too low to detect (by Ti 2p XPS) or is lost in the background of the signal from the majority of the Ti atoms present (in Ti K-edge EXAFS). The Pt core-level shift for the alloy state is small (4), and Ti is a weak scatterer of electrons relative to Pt, so that Pt L-edge EXAFS is dominated by Pt-Pt coordination. However, these problems in detectability can be circumvented by studying the chemical interaction between Pt and TiO_2 phases in an "inert" matrix. Here, the matrix is inert in the sense that it does not react directly with either phase itself. The changes in Ti chemistry are then easily followed, but there is a loss in direct applicability to the real Pt on TiO_2 catalyst system.

We have chosen to use carbon black as the inert matrix for this study rather than one of a variety of non-SMSI oxides (5) one might have chosen for this purpose. Many of the possible oxides do react with TiO_2 to form ternary oxides, and Pt is more mobile on carbon black than on

oxides thereby enhancing the rate of the interphase reaction under study. The chemical state of the Ti and the identification of phases present was made using a combination of XPS, EXAFS, and conventional x-ray powder diffraction (XRD). These characterizations showed unambiguously the conversion of separate Pt and TiO_2 dispersed phases into Pt-Ti alloy phases at progressively higher heat-treatment temperatures, eventually resulting in the formation of crystallites of the ordered (intermetallic) phase Pt_3Ti. Based on this observation, together with the conclusions of numerous recent reports of encapsulation of Pt supported on TiO_2, we present a model for the chemistry occurring during the formation of the SMSI state.

PREPARATION

All catalysts were prepared starting from a commercially available carbon supported Pt catalyst obtained from the Prototech Company (Newton Highlands, MA). The Pt loading of the material used was 10% by weight with a narrow particle size distribution of from 15-30 Å. TiO_2 was impregnated into the catalyst from aqueous solution by hydrolysis of $TiCl_4$. High purity (3N) liquid pure $TiCl_4$ was used as received from Alfa. A series of catalysts was prepared by addition of a calibrated volume of $TiCl_4$ to an agitated 1:1 methanol:water solution containing the Pt catalyst in suspension. The volume of $TiCl_4$ added was sufficient to yield about 1.5 wt. % Ti in the final catalyst, or about twice the stoichiometric amount for complete conversion of all Pt to Pt_3Ti. The catalyst was brought to dryness in an ultrasonic mixer. Large chunks of

catalyst were then ground with a mortar and pestle to obtain a fluffy fine powder we designate here as the as-prepared catalyst. Subsequent heat treatments were all run for 2 hours under flowing high purity He. The 700°C and 900°C heatings were done in a Pt boat, while the 1200°C heating was performed in a graphite boat.

INSTRUMENTATION

X-ray photoelectron spectroscopy (XPS) was performed in a Physical Electronics 548 Auger/ESCA system. The spectrometer uses a Mg K_α (1253.6 eV) x-ray source and a double-pass cylindrical mirror analyzer. The system is ion pumped with a base pressure following bake out of 4×10^{-8} Pa. Specimens were introduced into the analysis chamber by a rapid introduction probe. Binding energies were referenced to 83.8 eV for the Au 4f 7/2 photoelectron peak. For analysis the catalyst specimens were mixed with Teflon powder (10 wt%) as a binder and then pressed into a 5mm hole drilled through a 2cm x 1cm x 1mm aluminum holder. The aluminum holder was then mounted onto the probe tip. The data collection and analysis system used for XPS have been described elsewhere (6).

X-ray diffraction (XRD) was performed using Cu K_α radiation in a Siemens D-500 diffractometer. Powder specimens were held in a 2.5cm x 2.5cm x 1mm trough cut into the surface of a lucite block. Powders were pressed into the trough with a glass slide to obtain an even, smooth distribution of the powder.

X-ray fluoroscence (XRF) spectra were collected with a Tracor X-ray

Spectrace 4020. An Itel 8086 microprocessor controls data acquisition and analysis. A Rhodium x-ray source and a Si(Li) detector are used for excitation and collection of the fluorescence data.

Extended x-ray absorption fine (EXAFS) structure experiments were performed on the new beamline VI at SSRL. The experiments were performed with beam conditions of 3 GeV and 60 ma. The powders were mounted on a porous graphite substrate again using Teflon as a binder. The EXAFS specimen holder and fluorescence detector was obtained from F.W. Lytle (7). Fluorescence detection was chosen owing to the superior S/N capability in the analysis of metals in the highly dispersed state (8). Data evaluation was performed using software provided by Sandstrom (9).

RESULTS

1. XPS Analysis

X-ray photoelectron Spectroscopy was employed to identify the chemical state of the Ti as a function of heat-treatment. Titanium (2p), platinum (4f), carbon (1s), and oxygen (1s) photoelectron spectra were collected from each specimen. Survey scans were also collected to observe the presence of any contaminants. Bulk polycrystalline Pt_3Ti was analyzed to obtain standard Ti(2p) and Pt(4f) binding energies for the alloyed state, while the Ti(2p) and Pt(4f) binding energies for TiO_2 and metallic Pt were obtained from oxidized Ti foil and Pt foil, respectively. Binding energies of TiC, TiO and $TiCl_3$ were obtained by analysis of these powders mixed with graphite. A summary of the binding energies for these standard compounds is given in Table 1.

Titanium spectra from the catalysts are shown in Fig. 1. With increasing temperature the peak characteristic of intermetallic Ti (ca. 455 eV) grew dramatically. Titanium to platinum atomic ratios calculated from fitted XPS spectra quantitatively represent the changing form of the titanium (Table 2). As temperature increased the intermetallic Ti to Pt ratio rose to a level equal to that of the TiO_2 to Pt ratio, as expected, since twice the stoichiometric amount of Ti for formation of Pt_3Ti was used in the preparation. A more surprising observation is the apparent "loss" of total Ti on going from the as-prepared to the 700°C specimen. We know from the XRF elemental analysis that Ti is not lost in heat-treatment. The apparent "loss" indicated by XPS data can be explained in terms of the relative escape depths of the Ti and Pt photoelectrons, making certain assumptions about the distribution of TiO_2 in the catalyst matrix following impregnation. The Ti(2p) photoelectrons have lower kinetic energy, and thus shallower escape depth, than the Pt(4f) photoelectrons. If it is assumed that impregnated TiO_2 is deposited preferentially on the "exterior" of carbon aggregates (containing Pt uniformly dispersed), then the apparent "loss" can be rationalized in terms of Ti diffusion into the "interior" of carbon aggregates and resultant attenuation of Ti(2p) photoemission (relative to the uniformly distributed Pt). In this context, "interior" and "exterior" refer to geometries relative to electron energy analysis, i.e. as "seen" by the spectrometer.

The platinum spectra had small but reproducibly observable changes in response to the heat treatments. In all cases, deconvolution of the

Pt(4f) spectra indicated the presence of a minor Pt state with a binding energy ca. 2.5 eV higher than the metallic peaks as indicated by Fig. 2. While we have not assigned this state to a specific Pt compound, it is clear that this state is not related to the formation of the intermetallic phase. The Pt(4f, 7/2) binding energies exhibited small (< 0.5 eV) shifts with successive heat-treatment which we interpreted in the following manner. Initially the Pt is in a mixed valence state with chemisorbed oxygen or possibly a surface oxide giving rise to the high binding energy component (10). After 700°C heat treatment, the adsorbed oxygen is removed and/or the oxide is reduced, leaving the Pt mostly as metal. Upon further heating to 900 and 1200 degrees, significant alloying occurs causing the shift of the Pt(4f, 7/2) binding energy to a value indicative of Pt in Pt_3Ti.

Observed impurities were sulfur, chlorine, and oxygen. Sulfur and oxygen have been found to be impurities in the carbon support. Chlorine, due to the $TiCl_4$ starting material, is a significant impurity in the as-prepared specimen, e.g. 3.2 at %. Upon heating to 700°C, most of the chlorine is lost leaving only 0.5 at %. Catalyst composition (in at %) determined by XPS is listed below for the as-prepared catalyst:

C - 88.67%	O - 0.58%
Cl - 3.20%	S - 0.75%
Pt - 0.92%	Ti - 0.58%

X-ray fluorescence (XRF) analysis was performed to obtain an

indication of the total elemental Pt/Ti ratio. Prior to heat treatment the observed Pt to Ti ratio was approximately one-half that of a Pt_3Ti standard. This was as expected considering the two-fold excess Ti present in the catalyst preparation. Upon heat treatment to 1200°C the ratio dropped to approximately one-third that of the Pt_3Ti standard. The drop in the Pt/Ti ratio cannot be due to attenuation of the low energy x-rays by the larger particle size in the 1200°C sample since the lower energy Ti(K_α) photons would be attenuated to a greater extent causing an increase in the ratio. The most likely cause is platinum volatilization as a chloride or oxide as many of the possible Pt oxides and chlorides are volatile at temperatures above 600°.

2. XRD Analysis

X-ray diffraction is a powerful technique for the determination of crystalline structure and particle size of dispersed phases. The ordered alloy Pt_3Ti has an fcc structure (Ll_2, Cu_3Au type) with a_o = 3.906. We know from the XPS data that a significant fraction of the Ti persists as TiO_2. Figure 3a shows the diffraction pattern from the as-prepared specimen, very broad Pt and graphite reflections are observed. The absence of TiO_2 reflections in any of the diffraction patterns indicates that the TiO_2 must be amorphous. Lattice parameter values, summarized in Table 3, decreased from the as-prepared 3.926 Å to 3.906 Å for the 1200°C heat treated catalyst. Particle size calculated from the linewidths of the (111) reflections indicate a rapid jump from 48 Å to 110 Å upon heating to 700°C, then more slowly to 140 Å after 1200°C heat treatment. For both the 900 and 1200°C heat treated catalysts, superlattice lines

were observed, indicative of the formation of the ordered alloy phase. The relative intensity of superlattice lines is indicated by the scan shown in Fig. 3b. Calculation of the order parameter (11) indicated the 900°C catalyst to be 67% ordered, assuming the 1200°C catalyst was fully ordered.

3. EXAFS Analysis

Titanium K-edge EXAFS data were analyzed to follow changes in the nearest neighbor configuration around Ti atoms during heat treatment. Because EXAFS is caused by electron backscattering, the spectra are very sensitive to changes in coordination as dramatic as would occur in the transition from an oxide to an alloy due to the large differences in scattering cross-section between O^{2-} and Pt (or even between Ti and Pt). For the characterization of supported catalyst, EXAFS has an important advantage over XPS for chemical state determination in that it is a bulk technique, i.e. there is no screening of x-ray fluorescence from Ti "buried" in the carbon support, as is the case for photoemission. In analyzing the EXAFS data, we used a combination of the "fingerprint" method with $\chi(k)$, and quantitative analysis using the radial structure functions derived from the Fourier transform of $k^3\chi(k)$. The $\chi(k)$ spectra of the catalysts are compared directly to those for the standard compounds TiO_2, TiC and Ti metal as shown in Fig. 4. The spectrum for the 1200°C heat-treated catalyst is virtually identical to that from a Pt_3Ti crystal, and the spectrum for the catalyst prior to heat-treatment is virtually identical to that for TiO_2. After 700 and 900°C heat-treatment, there are features that are very common to both the TiO_2

and Pt_3Ti state. TiC has oscillatory features very similar to those for Pt_3Ti, which is expected since the Ti-Ti bond distances (second coordination shells) are close to those for Ti-Pt in Pt_3Ti. Fourier transform analysis of the $\chi(k)$ data for TiC indicated that scattering from the C atoms was not resolvable, i.e. the $\chi(k)$ is made up entirely of scattering from the Ti containing coordination shells. However, the amplitudes of the oscillations are four times larger in Pt_3Ti than in TiC, due to the higher scattering cross-section of Pt. The feature at $k \simeq 5$ and the three relatively strong oscillations for $9 < k < 12$ (relatively weak in TiC) are characteristic of the Pt coordination about Ti, and these features are clearly evident in the 900°C sample, and even discernable in the 700°C sample. In the 1200° sample, there appears to be no contribution from the unreacted TiO_2 (and observed to be present by XPS). As was the case for scattering from C atoms in TiC, scattering from oxygen nearest neighbors has a much lower amplitude contribution than scattering from Pt nearest neighbors, and the unreacted TiO_2 signal is lost in comparison to the signal from those Ti atoms that have formed the Pt_3Ti phase.

The Fourier transform of $k^3\chi(k)$ spectra are shown in Fig. 5. The magnitude of the Fourier transform contains peaks at distinct values of radial distance from the absorbing atom (in this case titanium). The peaks are not actually located at k-values corresponding to the true interatomic distances, but are shifted by a few tenths of Å due to a phase-shift when the photoelectrons are backscattered (12). The height of the peak is proportional to the number of atoms at that radial

distance (coordination shell) and to the electron scattering cross-section of these atoms (12). There is an attenuation of the contribution of back-scattering of atoms with radial distance, which causes the peaks to decrease in height with radial distance even if the coordination number were constant (12). For Ti in TiO_2, the first nearest neighbors are O atoms at 1.92 Å, and the second shell contains Ti at 2.99 Å (13). In the transform of the "as-prepared" spectrum, there are three peaks, one below 1 Å, one at 1.616 and one at 2.729 Å. The "peak" at < 1 Å is a "noise" feature caused by truncation of the $\chi(k)$ data at a finite value of k, and the latter two peaks correspond to Ti-O and Ti-Ti coordination in TiO_2, as expected. In Pt_3Ti, Ti atoms substitute for Pt at the corners of the fcc unit cell, with a_o = 3.906 Å. Therefore, the first coordination shell for Ti contains 12 Pt atoms at 2.762 Å, the second 6 Ti atoms at 3.906 Å, the third 24 Pt atoms at 4.784 Å. Since Ti is a much weaker scatterer of electrons than Pt, we would expect the second coordination peak to be weak relative to either the first or third. The transform of the 1200°C spectrum shows two strong peaks at 2.649 Å and 4.916 Å, consistent with these expectations for the Pt_3Ti structure. For the two spectra at the intermediate temperatures of 700 and 900°C, there is a progressive decrease of the Ti-O bond peaks and growth of the two Ti-Pt bond peaks. The Fourier transform analysis of the EXAFS spectra are, therefore, consistent with the "fingerprint" analysis of the X(k) spectra given above, and with the XPS and XRD analyses as well.

DISCUSSION

In the presence of a two-fold excess of TiO_2, dispersed Pt metal was found to be completely transformed into Pt_3Ti following heating to 1200°C under helium. Even at temperatures as low as 700°C, some alloying was detected. It is interesting to note the absence of TiC as an intermediate phase forming in the reduction of TiO_2. While this reaction might be expected intuitively, the reduction of TiO_2 by carbon in an inert atmosphere is not very favorable from a thermodynamic standpoint. Using the JANAF Thermochemical Tables, one finds that considering the equilibria

$$TiO_2 + 2C = TiC + CO_2$$

$$TiC + O_2 = TiO_2 + CO_2$$

the equilibrium partial pressures of oxygen and/or CO_2 for carbide formation are impractically low, considering that the carbon black we are using contains ca. 5 at % oxygen, and the inert gas at least a few ppm oxygen. If the equilibria are changed to reflect the formation of Pt_3Ti as the reduced state instead of TiC, the equilibrium pressures for oxygen and/or CO_2 become more realizable, since the free energy of formation of Pt_3Ti is ca. 100 kJ/mol more negative than for TiC. In practice, the actual reducing reactions are not known, but considering that the carbon

actual reducing reactions are not known, but considering that the carbon black contains significant levels of hydrogen and oxygen, and the inert gas contains some level of oxygen, the most probable reactions are:

$$TiO_2 + 2\ H_2 + 3\ Pt = Pt_3Ti + 2\ H_2O$$

$$TiO_2 + 2\ CO + 3\ Pt = Pt_3Ti + 2\ CO_2$$

where the equilibrium favors the formation of intermetallic if CO/CO_2 > 20:1 and/or H_2/H_2O > 20:1 (at 1100 K).

Other possible reduction products would be sub-oxides of TiO_2, for example TiO and Ti_3O_5. The thermodynamic favorability of formation of these solid phases may be compared to that for alloy formation by calculation of the reducing atmosphere partial pressure ratios required for their formation (Table 4). Compared to the thermodynamics for the formation of the intermetallic, the reduction of the TiO_2 to a suboxide is much less favorable. It is quite likely that the partial reduction of the TiO_2 will create small concentrations of various "sub-oxides" as intermediates; however, the energetics favor complete reduction and alloying to Pt_3Ti given sufficient temperature and time. Horsley's suggested model of Pt-$(TiO_6)^{-8}$ bonding could very well be the first step in the reduction of the TiO_2, as indicated by the XPS data of Fung (14) for hydrogen reduced Pt/TiO_2.

The results of this study provide definitive evidence that alloy formation occurs when Pt and TiO_2 are in contact and heated in a reducing

atmosphere. It is certain that alloy formation will occur in various Pt/TiO_2 phase configurations provided the atmosphere is sufficiently reducing and the temperature is high enough (at least 700°C). The temperatures at which we observed the onset of alloy formation was approximately 200°C higher than the usual SMSI reduction temperature (500°C). This higher temperature could be due to the fact that impregnation of TiO_2 in the Pt/carbon does not necessarily result in physical contact between Pt and TiO_2 phases, and a higher temperature is necessary to promote Pt migration to "find" the TiO_2. Nonetheless it is not clear that alloy formation is to be expected when Pt dispersed on TiO_2 is reduced at 500°C. However, together with our previous studies of the formation/dissolution of TiO_x overlayers on Pt_3Ti (15) and the chemisorptive properties of Pt_3Ti (16), the present results enable us to put together a new picture of SMSI chemistry that is consistent both with the characteristics of the SMSI state (1) and with recent results interpreted as "encapsulation" of Pt by TiO_x (17-22). The chemistry we have derived is shown in Fig. 6, both for Pt dispersed on TiO_2 powder and for Pt thin films. In the latter case, the model we give here is consistent with the report by Belton, et al. (22) that TiO_x ($x \simeq 1$) moieties are observed "on-top-of" Pt after high temperature annealing of Pt films on TiO_2 substrates, which they interpreted as "encapsulation" caused by migration of TiO_x moieties onto the Pt. We suggest that "encapsulation" of the Pt by migrating TiO_x moieties does not actually occur. Rather TiO_2 reduction occurs locally around Pt crystallites simultaneously with alloy formation; the alloy phase becomes imbedded in

a TiO_x (x≈1) matrix as a consequence of the counter diffusion of Pt and Ti atoms that occur with these simultaneous processes. The imbedding of the alloy phase causes the Pt/Ti surface ratio to decrease, and "TiO" character to appear at the surface, phenomena which Belton, et al. had interpreted as migration of "TiO" moeties onto the Pt surface. However, the chemistry of alloy formation, as shown in Fig. 6, also accounts for these spectroscopic results without invoking migration of "TiO" moieties (a difficult physical concept). Further, this picture is consistent with the CO adsorption results of White and co-workers (22-24) for Pt films on TiO_2 (and the effect of thermal annealing) whereas the "encapsulation" concept does not. We found in our study of CO chemisorption on Pt_3Ti that CO is less strongly bound on Pt_3Ti than on Pt, with a TDS desorption peak temperature for Pt_3Ti 40-50^oC lower than for pure Pt. A similar shift in TDS peak temperature of ca. 40^oC was reported by Belton, et al. (22). Tanaka and White (24) investigated CO stretching frequencies for CO adsorbed on Pt/TiO_2 catalysts. Upon high temperature reduction, they observed a preferential loss of a CO stretching frequency they attributed to CO bound at step sites on Pt. We suggest this shift could also be interpreted as loss of CO bound at Pt-Pt bridge sites due to the formation of Pt_3Ti, since we have shown (16) that the structure of the surface of Pt_3Ti is such that Pt-Pt bridge bonding sites are missing. The model in Fig. 6 also accounts for the observation of an overall decrease in the volume of CO adsorbed in the SMSI state, since the exposed area of Pt_3Ti is much lower than the original Pt area. The model is consistent with the changes in the Pt crystallite morphology observed

by Baker, et al. (25) with electron microscopy of Pt/TiO_2 catalysts subjected to high temperature reduction. They reported the apparent "spreading" of Pt into thin "pillbox" structures, which we suggest is the formation of the alloy phases concurrent with local TiO_2 reduction, i.e. "spreading" of Pt is actually Pt-Ti interdiffusion in alloy formation. As we have shown in our study of the oxidation of Pt_3Ti (15), heating Pt_3Ti in oxygen will cause the formation of separate Pt and TiO_2 phases in contact, i.e. heating the systems on the right hand of Fig. 6 restores the original Pt/TiO_2 phases, consistent with the reversibility of the SMSI state.

We do not suggest that Fig. 6 depicts the only SMSI state, but rather it is the thermodynamically favored state if the reduction conditions of the starting Pt/TiO_2 are sufficiently strong. Intermediate states consistent with the chemistry illustrated in Fig. 6 are easily envisioned, where the basic reactions occurring to form the alloy start but the reduction process is incomplete, e.g. Horsley's model (3) of Pt atoms bonded to Ti^{3+} centers is consistent with this chemistry.

ACKNOWLEDGMENT

This work was supported by the Assistant Secretary for Fossil Energy, Office of Fuel Cells, Advanced Concepts Division of the U.S. Department of Energy under Contract No. DE-AC03-76SF00098.

Table 1. Binding Energies[a] for Pt and Ti in Standard Compounds and Chemical Shifts.

	Pt(4f, 7/2)	Ti(2p,3/2)	Δ B.E.
Pt foil	70.9		ref.[b]
Pt_3Ti	71.2		+0.3
Ti foil		453.8	ref.[b]
TiO		454.6	+0.8
TiC		454.7	+0.9
$TiPt_3$		455.1	+1.1
TiO_2		458.5	+4.7
$TiCl_3$		459.4	+5.6

[a]Binding energy scale referenced to Au (4f, 7/2) at 83.8 eV.

[b]Reference state for chemical shifts.

Table 2. Integrated XPS Intensity Ratios of Ti(2p, 3/2) to Pt(4f, 7/2). Signals for Heat-Treated Catalysts.

Chemical State of Ti	As Prepared	700°C	900°C	1200°C
As TiO_2	1.89	0.49	0.48	0.47
As "alloy"	0	0.09	0.22	0.55
Total Ti	1.89	0.58	0.70	1.02

Table 3. XRD Analysis of TiO_2 Impregnated Pt on Carbon Catalyst Following Heat-treatment to Higher Temperature.

Catalyst	Lattice Parameter	Particle Size	Super-lattice
As-prepared	3.926 Å	48 Å	No
700°C	3.916 Å	110 Å	No
900°C	3.907 Å	125 Å	Yes
1200°C	3.906 Å	144 Å	Yes

Table 4. Thermodynamics of TiO_2. Reduction in H_2 or CO at 1100°K.

Reaction	Partial Pressure Ratio for Suboxide Formation
$TiO_2 + CO \rightarrow TiO + CO_2$	$CO/CO_2 > 3 \times 10^5$
$3\ TiO_2 + CO \rightarrow Ti_3O_5 + CO_2$	$CO/CO_2 > 10^6$
$TiO_2 + H_2 \rightarrow TiO + H_2O$	$H_2/H_2O > 3 \times 10^5$

References

1.) S. Tauster, S. Fung and R. Garten, J. Am. Chem. Soc., 100 (1978) 170.

2.) L. Brewer, in Phase Stability in Metals and Alloys, P. Rudman, J. Stringer and R. Jaffee, eds., McGraw-Hill, New York, 1967, pp. 39-61.

3.) J. Horsley, J. Am. Chem. Soc., 101 (1979) 2870.

4.) G. Derry and P. Ross, Sol. State Commun., 52 (1984) 151.

5.) S. Tauster and S. Fung, J. Catal., 55 (1978) 29.

6.) B. Beard, D. Dahlgren and P. Ross, J. Vac. Sci. Tech. A, in press.

7.) F. Lytle, R.B. Greegor, D.R. Sandstrom, E.C. Marques, J. Wong, C.L. Spiro, G.P. Hoffman and F.E. Huggins, Nucl. Inst. and Meth., 226A (1984) 542.

8.) J. Hastings in EXAFS Spectroscopy, Techniques and Applications, B.K. Teo and D.C. Joy, eds., Plenum Press, 1981, Chapter 12.

9.) D.R. Sandstrom, Il Nuovo Cimento, Vol. 3 (1984) 825.

10.) T. Dickinson, A. Povey and P. Sherwood, J. Electrochem. Soc., Faraday Trans. I, 71 (1975) 298.

11.) B. Cullity, "Elements of X-ray Diffraction," Addison-Wesley Publishing, 1967, pp. 372-375.

12.) E. Stern, D. Sayers and F. Lytle, Phys. Rev. B, 11 (1975) 4836.

13.) Landolt-Bornstein, K. Hellwege and A. Hellwege, eds., Springer-Verlag, 1975, Vol. III, p. 761.

14.) S. Fung, J. Catal., 76 (1982) 225.

15.) U. Bardi and P. Ross, J. Vac. Sci. Technol. A, 2 (1984) 1461.

16.) U. Bardi and P. Ross, submitted to the Journal of Catalysis, 1985.

17.) P. Meriandeau, J. Dutel, M. Dufaux and C. Naccache in "Metal-Support and Metal-Additive Effects in Catalysis," B. Imelik, et al. eds., Elsevier, Amsterdam, 1982, pp. 95 ff.

18.) J. Santos, J. Phillips and J. Dumesic, J. Catal., 81 (1983) 147.

19.) D. Resasco and G. Haller, J. Catal., 82 (1983) 279.

20.) H. Sadeghi and V. Henrich, J. Catal., 87 (1984) 279.

21.) Y. Chung and S. Takatani, J. Catal., 90 (1984) 75.

22.) D. Belton, Y. Sun and J. White, J. Phys. Chem., 88 (1984) 5172.

23.) D. Belton, Y. Sun and J. White, J. Phys. Chem., 88 (1984) 1690.

24.) K. Tanaka and J. White, J. Catal., 79 (1983) 81.

25.) R. Baker, E. Prestridge and G. McVicker, J. Catal., 89 (1984) 422; R. Baker, E. Prestridge and R. Garten, J. Catal., 59 (1979) 253.

Figure Captions

Fig. 1. XPS spectra from Ti(2p) region as a function of heat-treatment temperature.

Fig. 2. XPS spectra from Pt(4f) region of standard Pt on carbon catalyst after air exposure.

Fig. 3a. X-ray diffraction scan of the TiO_2 impregnated standard Pt on carbon catalyst in the as-prepared state; 3b. Scan for the 1200^o heat-treated catalyst. Graphite (002) and (10) reflections are at ca. 25 and 43^o respectively. Superlattice lines are indicated. Cu-K radiation.

Fig. 4. Normalized EXAFS spectra for the standard compounds Ti (foil), TiC, TiO_2, and the TiO_2 impregnated Pt catalysts. Dashed lines denote features unique to the spectrum for a Pt_3Ti standard.

Fig. 5. Magnitude of Fourier transform of k^3 (k) spectra for the TiO_2 impregnated Pt catalyst as a function of heat-treatment temperature.

Fig. 6. Proposed model for chemistry occurring in the formation of the SMSI state for: (a.) TiO_2 thin films on Pt; (b.) Pt thin films on TiO_2 substrates; (c.) dispersed Pt on TiO_2 powder.

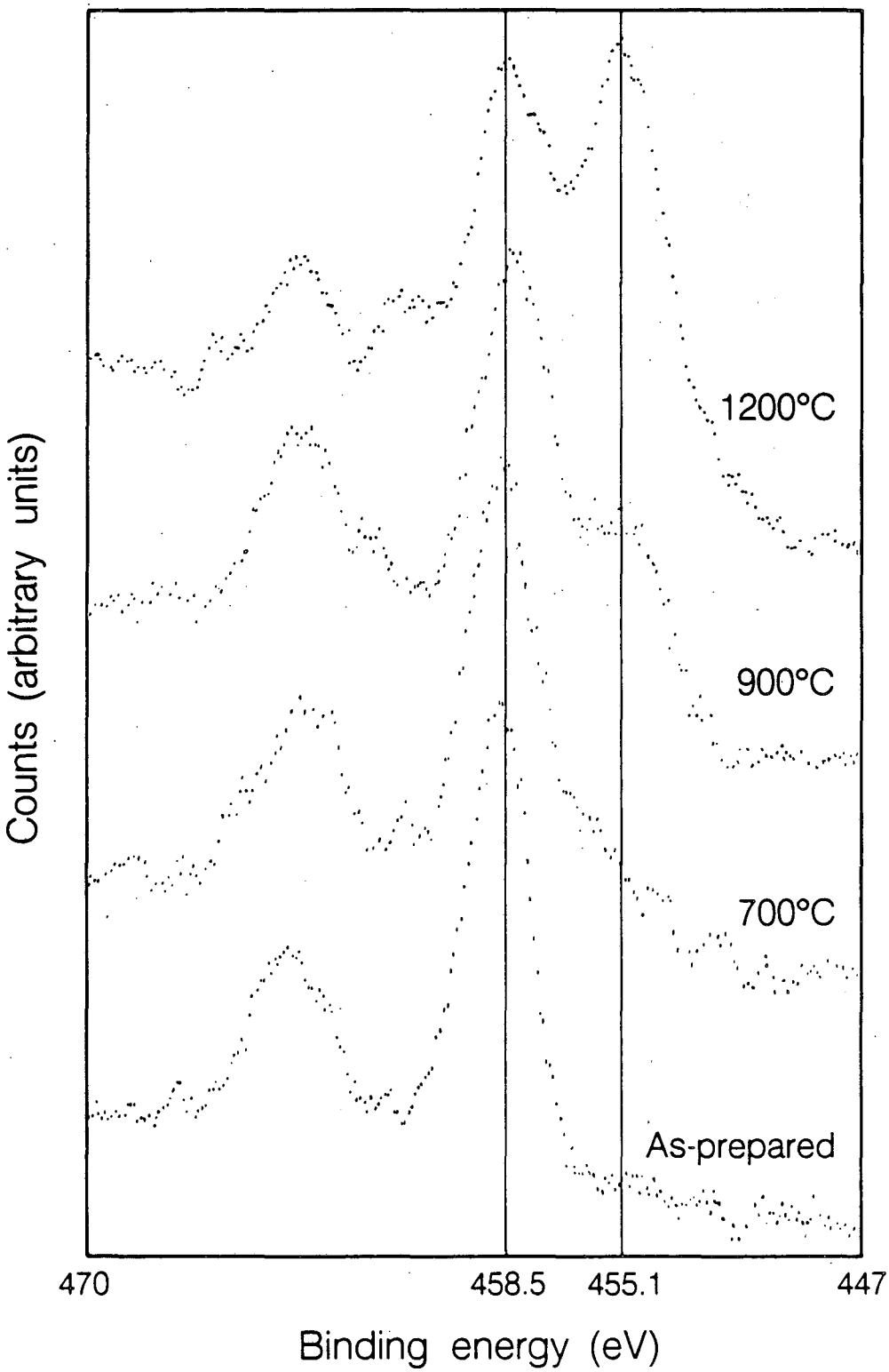

XBL 855-8896

Fig. 1

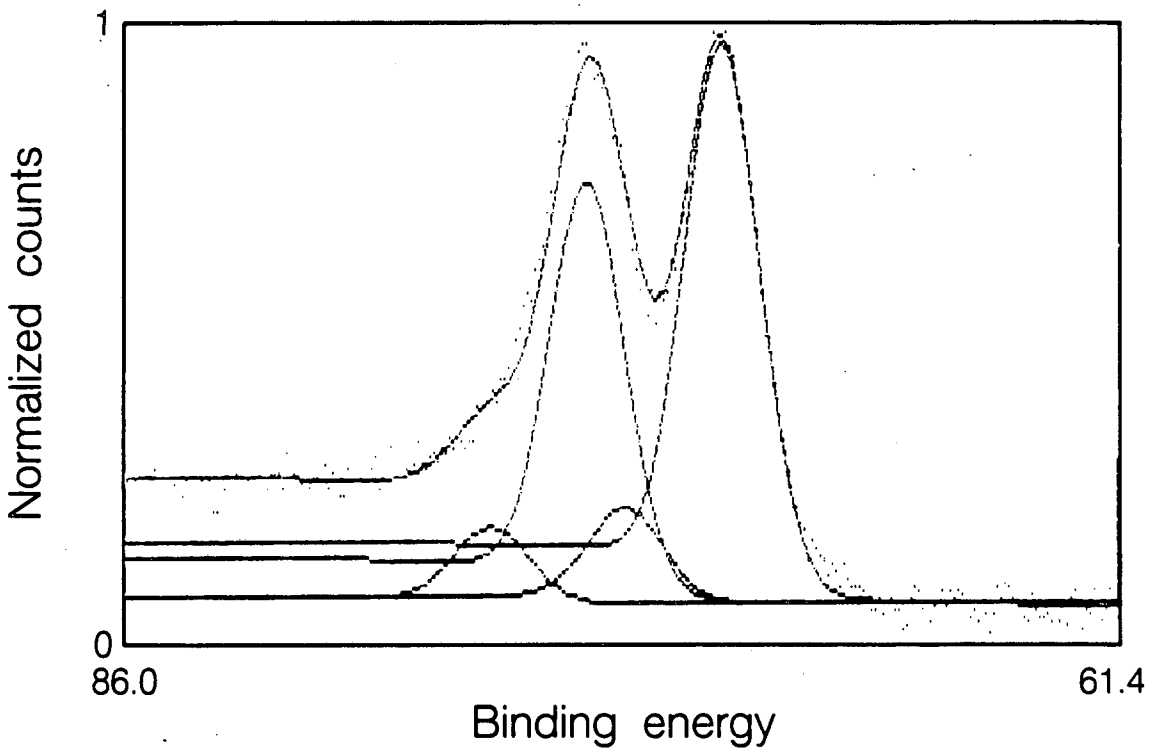

XBL 855-8897

Fig. 2

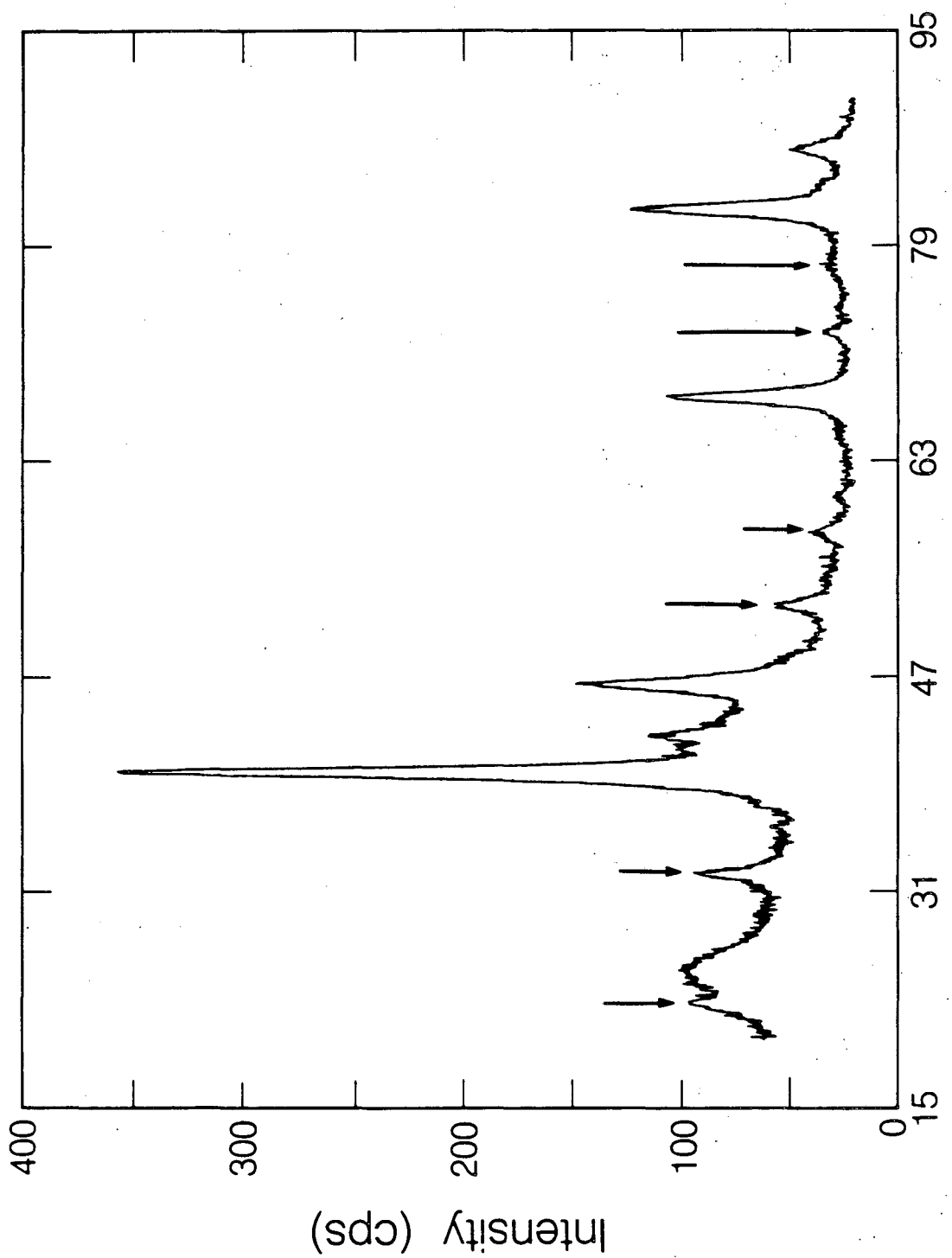

XBL 855-8895

Fig. 3a

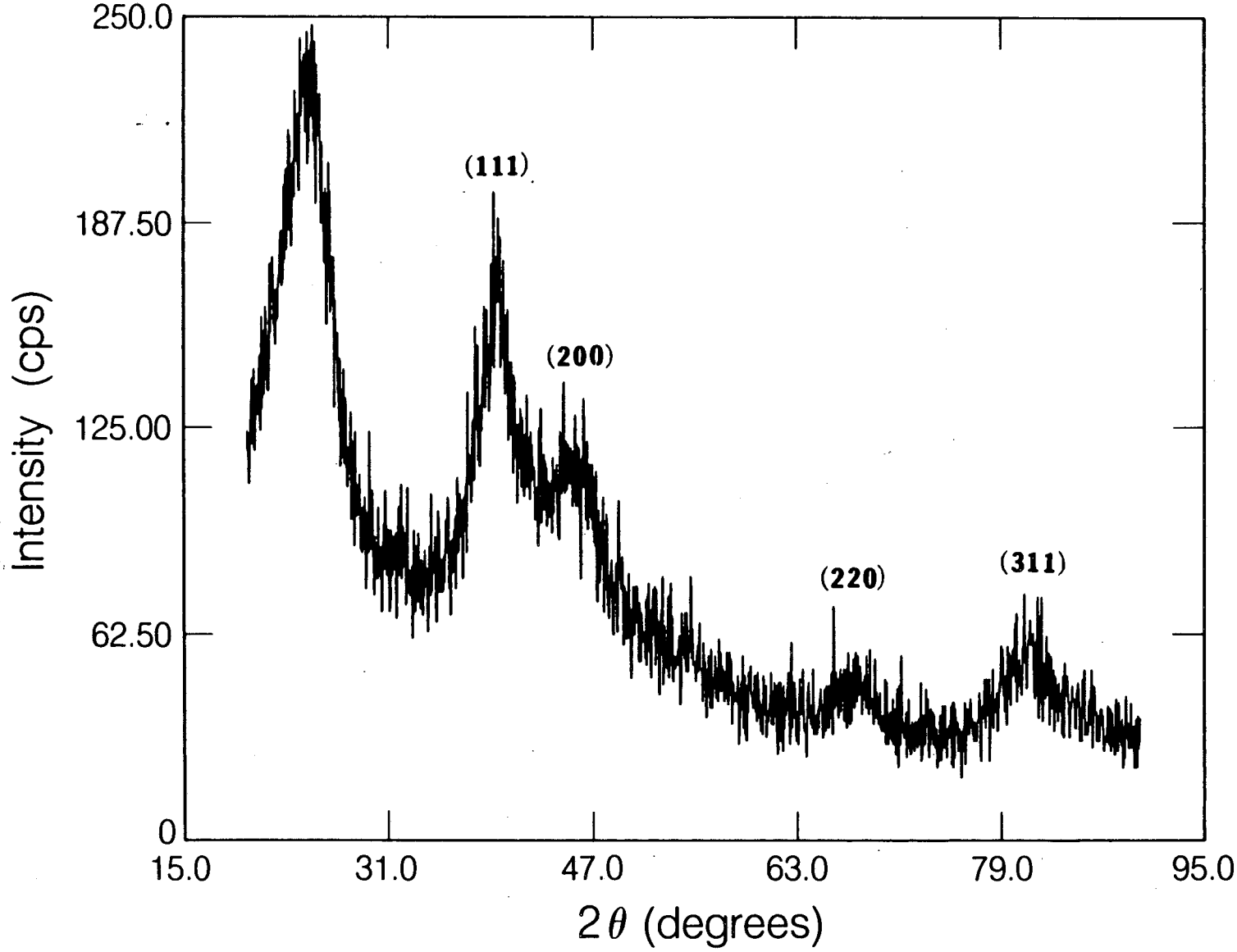

XBL 855-8894

Fig. 3b

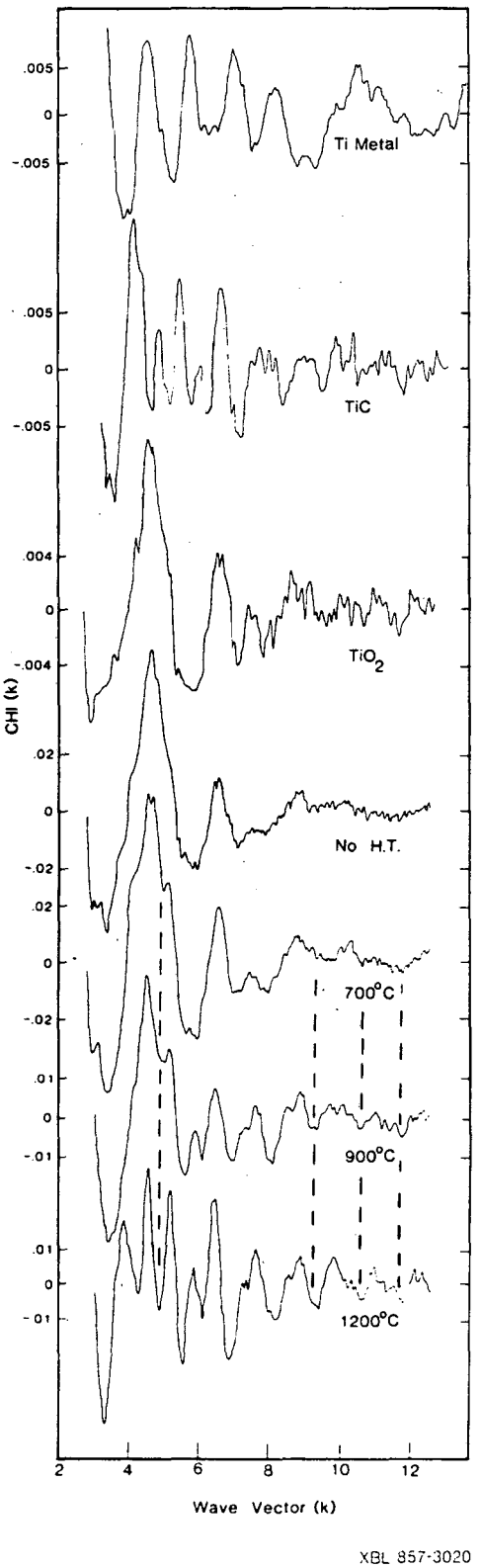

XBL 857-3020

Fig. 4

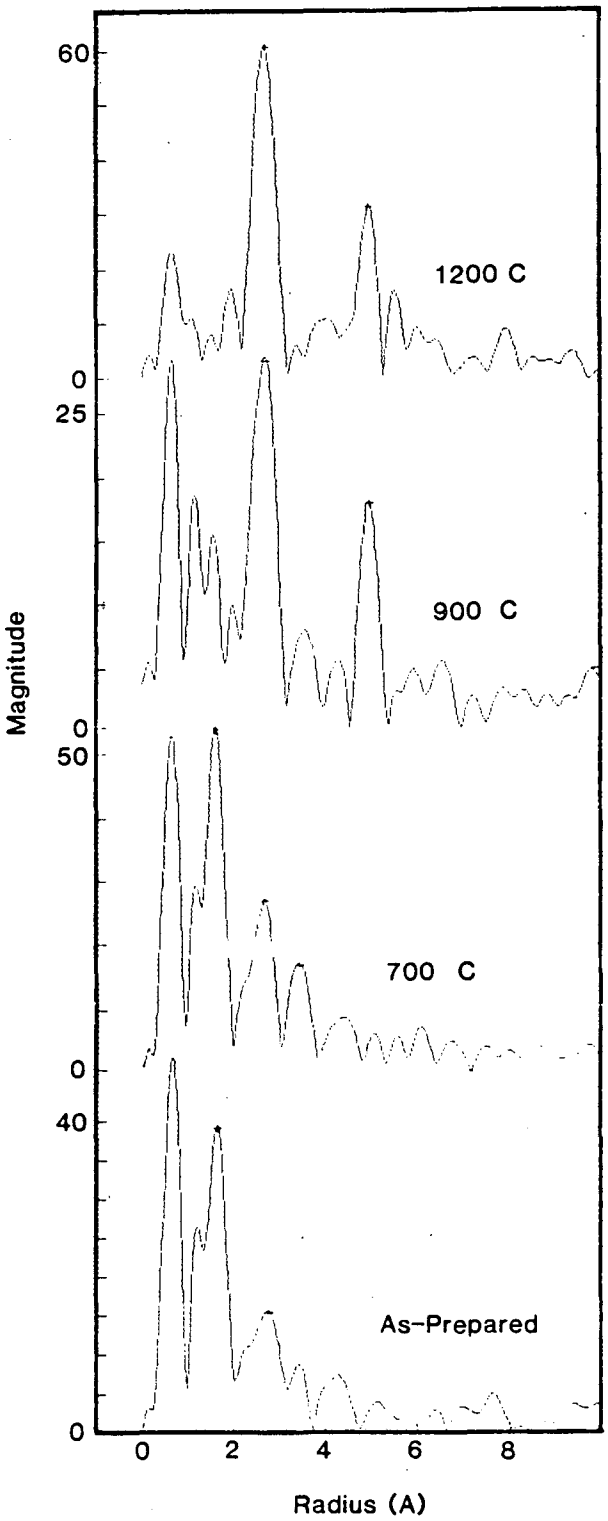
60
0
1200 C
25
0
900 C
50
0
700 C
40
0
As-Prepared
Magnitude
0
2
4
6
8
Radius (A)
XBL 857-3117

Fig. 5

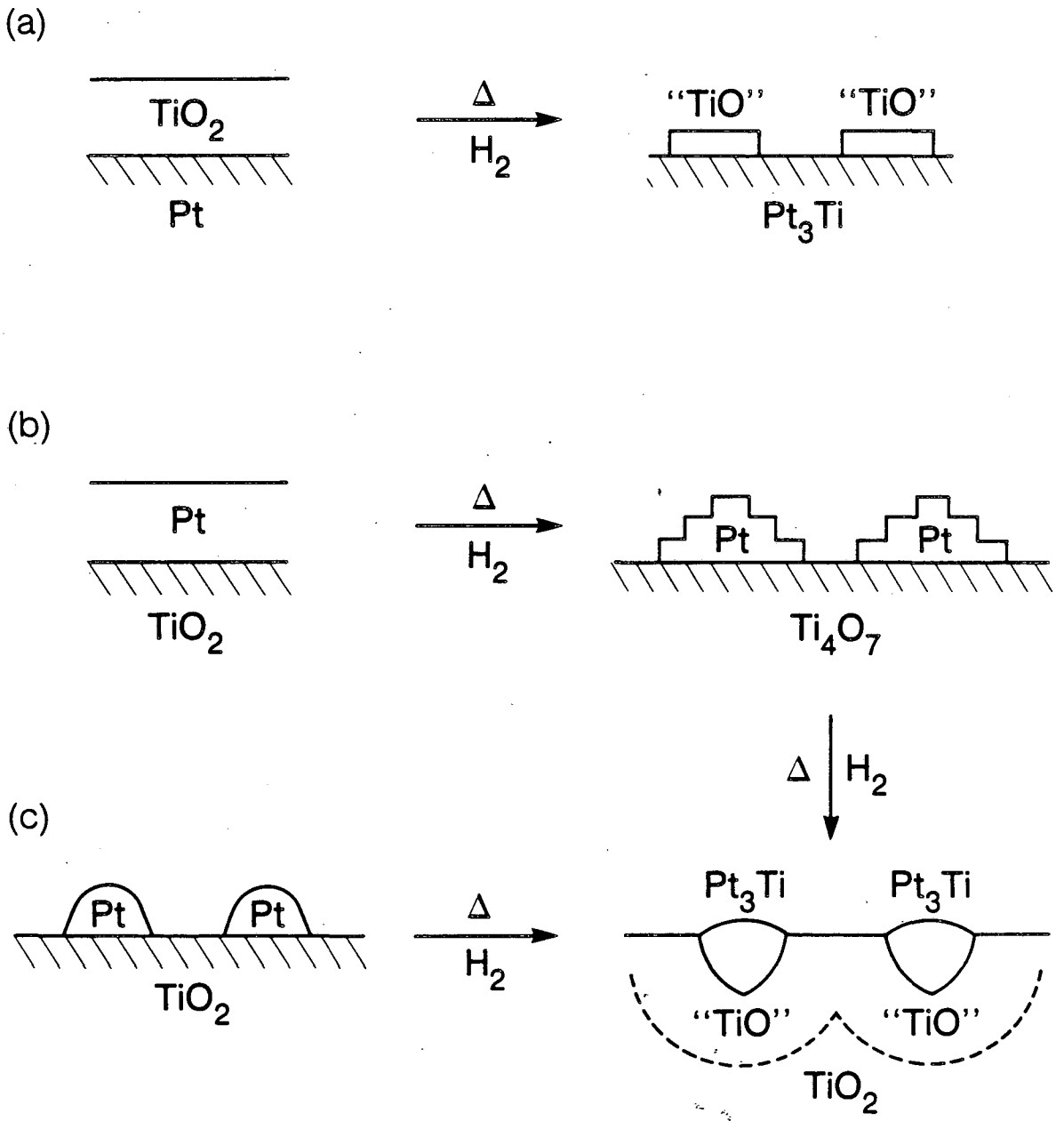

XBL 859-8988

Fig. 6

This report was done with support from the Department of Energy. Any conclusions or opinions expressed in this report represent solely those of the author(s) and not necessarily those of The Regents of the University of California, the Lawrence Berkeley Laboratory or the Department of Energy.

Reference to a company or product name does not imply approval or recommendation of the product by the University of California or the U.S. Department of Energy to the exclusion of others that may be suitable.

LAWRENCE BERKELEY LABORATORY
TECHNICAL INFORMATION DEPARTMENT
UNIVERSITY OF CALIFORNIA
BERKELEY, CALIFORNIA 94720